Some Progress on Interferometry Techniques Applied to Particle Measurements

Gérard Gréhan, Marc Brunel, Sébastien Coëtmellec, Annie Garo, Denis Lebrun, Siegfried Meunier-Guttin-Cluzel, Sawitree Saengkaew, Yingchun Wu, Xue Cheng Wu, Ling Hong Chen

Available online at www.sciencedirect.com

ScienceDirect

Procedia Engineering 102 (2015) 54 – 63

Procedia Engineering

www.elsevier.com/locate/procedia

The 7th World Congress on Particle Technology (WCPT7)

Some progress on interferometry techniques applied to particle measurements

Gérard Gréhan[1*], Marc Brunel[1], Sébastien Coetmellec[1], Annie Garo[1], Denis Lebrun[1], Siegfried Meunier-Guttin-Cluzel[1], Sawitree Saengkaew[1], Yingchun Wu[2], Xue Cheng Wu[2] and Ling Hong Chen[2]

[1]*CORIA-UMR 6614- Normandie Université, CNRS-Université et INSA de Rouen, , Campus Universitaire du Madrillet, St Etienne de Rouvray, 76800, FRANCE*

[2]*CEU, Zhejiang University, Hangzhou, China*

Abstract

The aim of this paper is to present some new developments in particle characterization. More precisely, the paper will be focused on the description of some progresses in the characterization of particles by interferometric methods which are generally considered as the most accurate ones. Three standard configurations will be presented and discussed: i) Interference between scattered light from a particle and a single reference beam (holography), ii) Interference between different kinds of light scattered by a single particle (ILIDS), iii) Interference between the light scattered from different particles. A special attention will be devoted to the possibility to obtain 3D information on the particle location.

Selection and peer-review under responsibility of Chinese Society of Particuology, Institute of Process Engineering, Chinese Academy of Sciences (CAS)

Keywords: Particle characterization; Lorenz-Mie theory, Holography; 3D imaging.

* Corresponding author.
E-mail address: grehan@coria.fr

Selection and peer-review under responsibility of Chinese Society of Particuology, Institute of Process Engineering, Chinese Academy of Sciences (CAS)
doi:10.1016/j.proeng.2015.01.106

Nomenclature

A_i, A_t	The amplitude scattered by one particle on a detector pixel, the total amplitude on a single pixel
DLS	Dynamic Light Scattering
FII	Fourier Interferometric Imaging
I_t	The total intensity on a pixel of the detector
ILIDS	Interferometric Laser Imaging Droplet Sizing
MSD	Mean squared displacement
MSDV	Mean squared distance variation
N	The number of particles in the control volume
PDA	Phase Doppler Anemometer
$\left\langle X_i^2 \right\rangle$	The mean squared displacement of the *i*th particle
$\left\langle X_{i,j}^2 \right\rangle$	The mean squared distance variation between particle *i* and *j*

1. Introduction

The characterization of the discrete phase of multiphase flows is still a challenge for fundamental studies as well as industrial applications. By characterization of particles we mean the measurement or the estimation of their size, velocity, shape, refractive index (i.e. temperature and composition), …

To characterize the discrete phase (the particles), a huge number of techniques exists based on different physical principles. If we focus on the optical techniques, they can be sorted in two large families: i) Techniques working on a single particle as Holography, PDA, imaging, ILIDS, standard rainbow refractometry, ... ii) Techniques giving an averaged information on a cloud section as diffractometry, global rainbow technique, turbidimetry, DLS….

Among these techniques, the most accurate ones are based on the use of interferences. These interferences can be between the different kind of light interaction with the particle as for ILIDS and Standard rainbow refractometry, between the light scattered from different sources as for PDA or between the scattered light and a reference beam as for holography.

Nowadays, the development of interferometric techniques to characterize single particle is an active field of research. Nevertheless, it is also possible to design section of cloud measurement based in the recording of the interference field. We expect that all the particles in a section of a cloud can be measured with the same accuracy than a single particle.

Accordingly this paper will be organized as follows. Section 2 will recall the measurement of inclusion inside a spherical droplet by holography. Section 3 will be devoted to recall the extension of ILIDS to the measurement of spherical particles 3D position as well as the characterization of irregular particles. Section 4 will be the introduction of FII to characterize directly a section of cloud by recording and processing the interference field in a given direction. Then practical applications to small or large particles will be described. Section 5 is a conclusion.

2. Interference between one particle and a reference beam

Basically, in particle measurement, holography is based on the recording of the interference fringes created by the scattered light interfering with a reference beam. The quality of the measurement (3D location, particle size, ..) is strongly connected to the knowledge of the reference beam. Accordingly, in the special case where we want to measure the properties of small particles embedded in a larger droplet, the reference beam as well as the illumination of the inclusion are unknown: the reference beam impinging on the detector depends on the droplet size and shape, the local light field on the inclusion depends both on the particle size and shape AND on the inclusion location inside the droplet. Nevertheless, we have recently developed an inversion strategy; based on 2 Dimensional FRactional Fourier Transform (2D-FRFT) which permits to process such images [1, 2, 3]. Figure 2.1 displays an

example of recorded hologram while figure 2.2 displays an example of reconstructed plane. In figure 2.1, on the right, the circular fringes correspond to the effect of the large droplet while the traces closer to the center correspond to the hologram of the inclusion inside this large droplet. Reconstruction of the hologram can then be realized using the 2D-FRFT [4, 5]. In figure 2.2 obtained after reconstruction of an hologram, four particles can be identified: two are in focus, two are out of focus. The two particles in focus are identified by a black circle. By using the fractional Fourier transform they have been located in the host water droplet at distance 14.4 mm from the CCD sensor. Moreover, each particle is represented by a spot and a long dash. This is due to a specific illumination scheme: a double pulse acquisition (short and long pulse) in order to identify the displacement direction [6]. The short pulse acts as a precursor. The small spot corresponds to the origin position of the inclusion. The long pulse allows then to observe the following part of the inclusion trajectory.

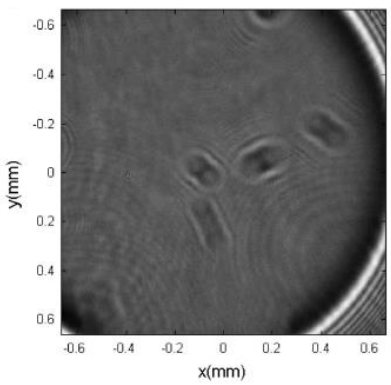

Figure 2.1: Example of in-line hologram of micronic inclusions in a spherical droplet

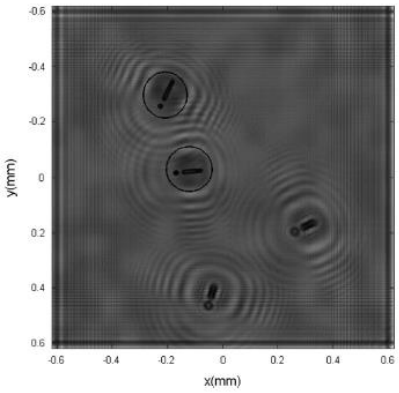

Figure 2.2: an optimal reconstructed plane within the droplet

3. Interference between the light scattered by one particle

ILIDS technique has been introduced by Glover et al. [7] to measure the droplet 2D position in a plane and the particle size in sparse cloud and free space. Its principle is to record the out of focus image of the light scattered by spherical droplet on which a laser sheet impinges (see figure 3.1). Then, on the recorder, each particle creates a circular image where vertical fringes code the size information. First a general simulator based on optical transfer matrices has been developed in order to describe a wide range of imaging configurations [8].

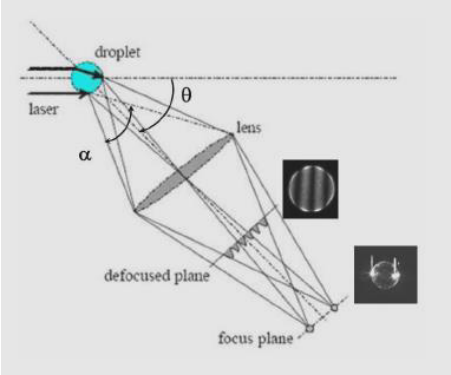

Figure 3.1: Typical set-up of ILIDS

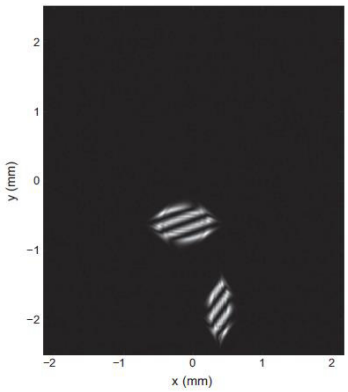

Figure 3.2: Out-of-focus pattern of spherical droplets in a cylindrical imaging system for 3D location of the droplets

We have then demonstrated (numerically and experimentally) that by adding the appropriate cylindrical lens, the third dimensional position of spherical droplet can be evaluated from the fringes rotation (see figure 3.2) [9]. These first experiments have been realized with droplets in air. Similar configurations have been performed to characterize bubbles in a liquid: water or glycerin [10, 11].

Moreover, the extension of ILIDS to the characterization of irregular particles has also been realized [12, 13]. In this case the basic experimental configuration is the classical one, but the processing is based on the 2D autocorrelation of the image. Figure 3.3 is an example of a ILIDS image for an irregular particle with its associated 2D autocorrelation. The interferometric out-of-focus pattern of the irregular rough particle is a speckle-like pattern. The size of the speck of light has been shown to be analytically linked to the size of the irregular particle. The size of the speck of light is obtained after a 2 Dimensional autocorrelation of the speckle-like pattern. The dimension of the central peak is then inversely proportional to the dimension of the particle [13].

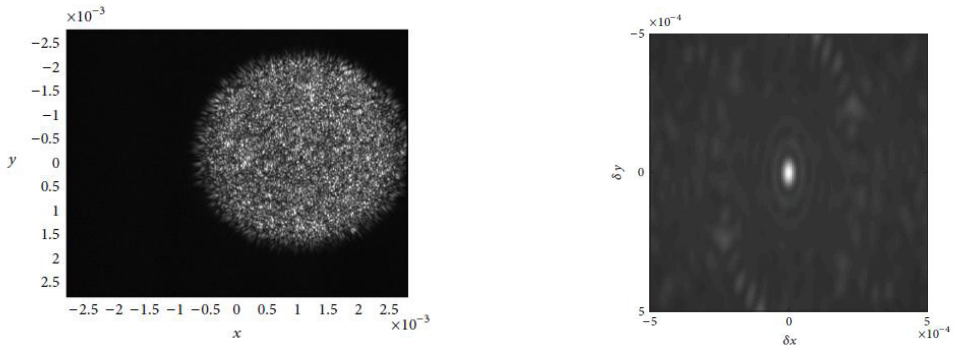

Figure 3.3 Typical Out-of-focus pattern of an irregular rough particle and the central peak of its 2D-autocorrelation

4. Interference between light scattered by several particles

Let us assume that the field of interference created by the light scattered from a section of a cloud on a detector surface is recorded. In this case, the amplitude on a single pixel of the detector is given by:

$$A_t = \sum_{i=1}^{N} A_i \tag{1}$$

where A_i is the amplitude of the light scattered by a single particle and N the number of particles in the control volume. Accordingly, the total intensity is:

$$I_t = A_t \bullet A_t^* = \sum_{i=1}^{N} A_i \bullet A_t^* + \sum_{i=1}^{N} \sum_{j=1|i\neq j} A_i \bullet A_j^* \tag{2}$$

The major novelty of Fourier Interferometric Imaging (FII) is to work with the $A_i \bullet A_j^*$ terms [14]. To do that, as exemplified in figure 4.1, the 2D FFT of the interference field is computed. Each trace in the 2D FFT corresponds to a term $A_i \bullet A_j^*$ which has the following properties:

1. The distance between a trace and the image center is directly proportional to the distance between the two particles constituting this pair,
2. The number of traces is given by the number of combinations 2 at 2 of the particles in the control volume, that is to say *N×(N-1)* where *N* is the number of particles in the control volume. This means that each particle can be measured up to *N-1* times on one recording.
3. The intensity of one trace is proportional to the square root of the product of both intensities scattered by each particle. The signal is no more proportional to d^2 or d^6 according if the particle is larger or smaller than the incident wavelength.

The processing of such images will depend on the size of the particles. When the particles are larger than the wavelength, the scattering diagram is complex as different 'kinds of light' issued from the same particle interfere together (i.e. externally reflected light, two times refracted light, two times refracted light with internal reflections). Accordingly, the parameters describing the particles can be extracted from each recorded interference field. On the opposite, for particles smaller than the wavelength, the scattering diagram is very regular and it is difficult to extract any information directly from the trace on a single recorded interference field. The information on the particle must be searched from the time evolution in a series of recorded interference fields due to the Brownian motion.

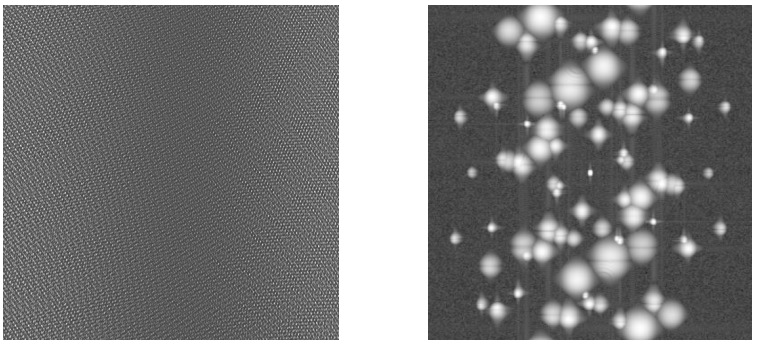

Figure 4.1: A typical interference field and its associated 2D FFT (computed for nano particles).

4.1) Particles larger than the wavelength

When the particles are larger than the wavelength, the size information is coded in the shape of trace. Accordingly, the trace will be processed. The processing, based on the properties of the 2D FFT, is schematized in figure 4.2. Starting from a recorded interference field, the 2D FFT is computed. It can be viewed as two matrices one for the real part, one for the imaginary part. From these two matrices, a magnitude matrix can be computed where the different traces of interaction can be identified. At an identified trace, it is possible to associate a mask with a transmittance of one for the trace and zero around. This mask can be applied to the real and imaginary matrices, and from the weighted matrices, by computing the inverse 2D FFT the scattering diagram corresponding to this pair of particles can be computed. From three interacting particles, the scattering diagram of each individual particle can be extracted, and processed to obtain its size and refractive index.

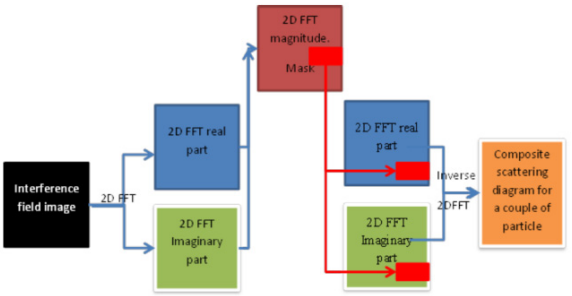

Figure 4.2: Schema of the FII image processing.

To prove the validity of the proposed approach a first series of experiments has been carried out with lines of monodispersed droplets, created by a droplet generator from the company FMT Technology Gmbh. Figure 4.3 displays a typical line of monodispersed droplets. From the image, taking into account the magnification, the droplets diameter is estimated to be equal to about 200 µm and the distance between particles to be equal to 400 µm. The droplet line was lighted by a laser pulse (wavelength 532 nm, duration 10 ns). The scattered light was simultaneously recorded by two cameras (Balster, 2048 x 2048 pixels). One camera was in forward scattering configuration (45°) while the second was in backward configuration (142°).

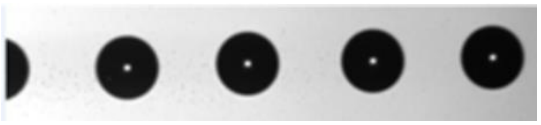

Figure 4.3: A typical line of monodispersed droplets.

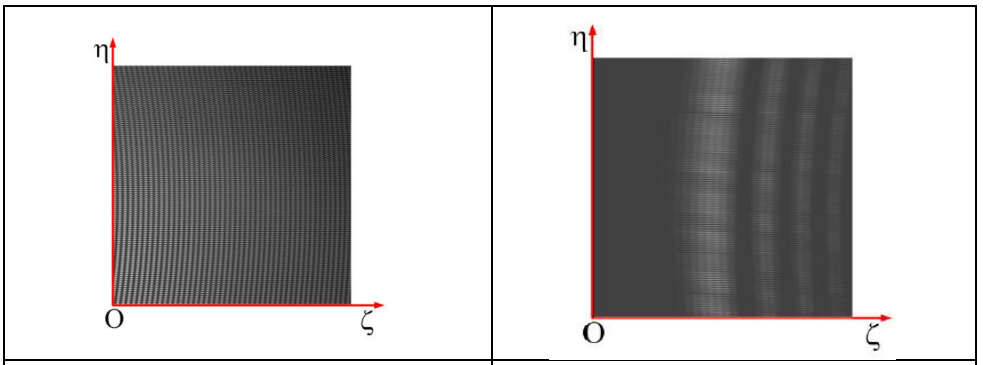

Forward interference field	Backward interference field

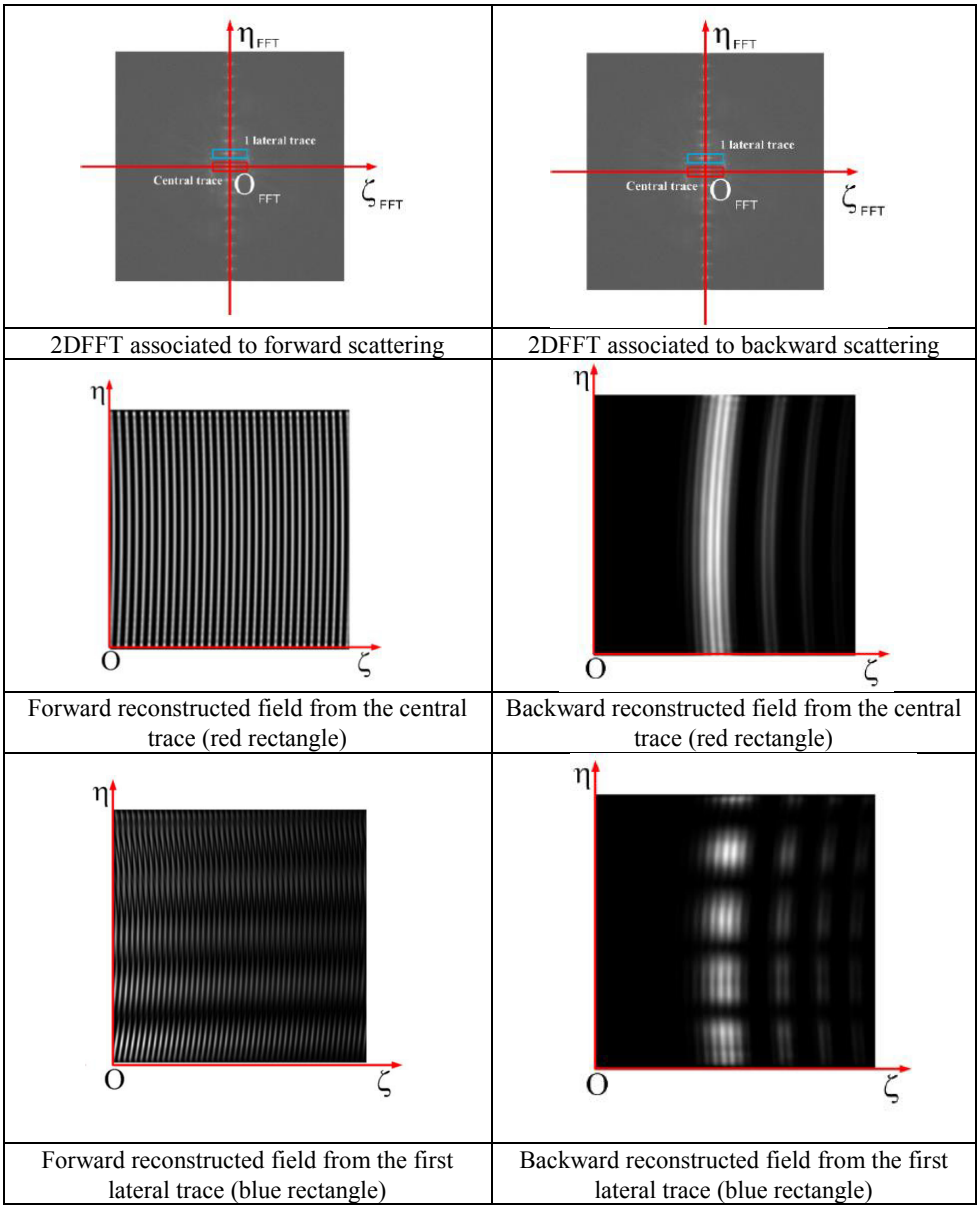

Figure 4.4: Comparison between forward and backward FII images processing.

The first line of figure 4.4 displays the recorded interference fields corresponding to forward or backward scattering. In the backward, the rainbow structure is easily recognizable.
The second line of figure 4.4 displays the associated 2DFFT of the interference fields. The 2DFFT associated to forward and backward scatterings are very similar.
Then the central 2DFFT trace and the first lateral trace are selected (identified by red and blue rectangles in the second line), and the mask corresponding to these traces is applied to the whole 2DFFT field and the inverse 2DFFT is computed. The results are displayed in line 3 and 4.

The figures displayed in line 3 correspond to the inverse 2DFFT of the central trace, then according to formula (2) to the summation of the intensities scattered by all the particles in the control volume. In the particular case of backward scattering, the signal is the global rainbow signal from which a mean refractive index and a size distribution can be extracted.
The figures displayed in line 4 correspond to the inverse 2DFFT of the first lateral trace: particles separated by one elementary step. On these two figures large interference bands are visible, corresponding to interference between particles with a small modification of the inter-particle distance. From such interference bands modifications smaller than one micron over 400 µm have been measured.

4.2) Particles smaller than the wavelength.

When the particles are smaller than the wavelength, the trace shape doesn't provide information about the size. The information on the size will then be extracted from the temporal behavior of the trace. In particle size measurement based on Brownian motion (tracking, DLS, ..), the mean squared displacement (MSD) is measured. The MSD is defined as:

$$\left\langle X^2(t)\right\rangle = \frac{\sum_{i=1}^{N}(x_i(t)-x_i(0))^2}{N} \tag{3}$$

In FII, the measurement is not the location of the particle but the distance between the two particles of a pair. Accordingly, the mean squared distance variation (MSDV) $\left\langle X_{1,2}^2\right\rangle$ is measured, which is related to the MSD by:

$$\left\langle X_{1,2}^2\right\rangle = \left\langle X_1^2\right\rangle + \left\langle X_2^2\right\rangle \tag{4}$$

To simulate an FII experiment, a Lorenz-Mie code predicting the interference field on a CCD detector in an arbitrary direction has been used [15, 16]. This code has been coupled with a numerical simulation of the Brownian motion to predict the displacement of the particles. With this code, the temporal behavior of a particles cloud has been simulated. The interference field has been computed for each time step. In this paper, the time step between two records is assumed to be equal to 0.01 second and 500 steps have been computed corresponding to a 5 seconds experiment. Then the 2DFFT of each interference field has been computed, and the location of the traces in the associated 2DFFT space has been measured for each time step, permitting to directly measure the MSDV.

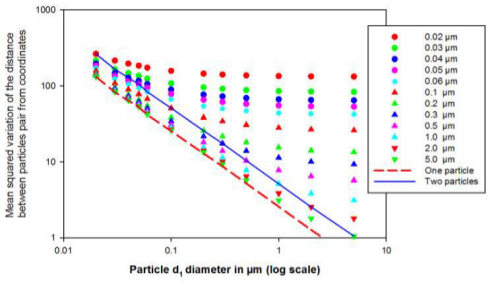

Figure 4.5: MSDV versus particle diameter.

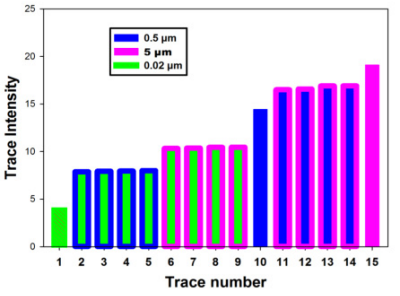

Figure 4.6: Trace intensity

Figure 4.5 plots the logarithm of the MSDV versus the logarithm of the diameter of one particle of a pair.

The studied parameter is the size of the second particle of the pair. Moreover, the MSD ($\left\langle X_1^2\right\rangle$) for the first

particle of the pair is plotted as a dashed red line as well as two times this value which is plotted as a blue continuous line. A first remark is that the blue line fits perfectly the MSDV measured for pairs of particles of the same size, verifying equation (2). A second remark is that when the particle pair consists in a large particle and a small particle, the MSDV corresponds to the MSD of the smallest particle. For example, for a pair with a 5 µm diameter particle (green triangles), the FII measures directly the MSD of the particles smallest than 0.2 µm.

Figure 4.6 plots the intensity versus the trace. For clarity reasons, only 6 particles of three different sizes have been selected for this figure: 2 particles of 0.02 µm, 2 particles of 0.5 µm and 2 particles of 5 µm. 30 traces correspond to that configuration (30 = 6 x 5). Taking into account the 2DFFT symmetry, the study can be limited to 15 traces. In figure 4.3, the bars with a uniform color (bar 1, 10 and 15) correspond to pairs with two identical particles. The intensity of the trace is identical to the intensity measured with classical imaging approach, that is to say proportional to d^6. The difference of intensities between the 0.02 µm and 5 µm particles is equal to 16 (in log units). On the contrary, the bar with two colors corresponds to trace for two different sizes of the particles (traces 2, 3, 4 and 5: pair 0.02 and 0.5 µm; traces 6, 7, 8 and 9: pair 0.02 and 5 µm; traces 11, 12, 13 and 14: pair 0.5 and 5 µm). Then to measure all the particles of this cloud it is sufficient to process the traces 2 to 9. For these four traces the difference of intensity is only 2 (in log units). This result demonstrates the efficiency of FII approach to increase the signals of the smallest particles.

Conclusion

The accurate measurement of single particle and particles fields is a challenge. In this paper, some recent progresses on the characterization of such configuration by interferometric techniques are reported. Examples are given for three configurations: i) Interferences between the scattered field and a reference field, ii) interferences between the different kinds of light scattered by a single particles, iii) interferences between the fields scattered by several particles. The advantages, disadvantages and originalities of each of these techniques are discussed.

Acknowledgements

The authors acknowledge the financial support of the French Agence Nationale de la Recherche (ANR), for the program NANOMORPH, through the program “Investissements d’Avenir”(ANR-10-LABX-09-01) , LabEx EMC^3, Genome-premices and European Program INTERREG IV-a E3C3. The European Community for the program INTERREG IV-a E3C3 as well as the National Natural Science Foundation of China (NSFC, grant 51176162), the National Science Fund for Distinguished Young Scholars (grant 51125025) and the Program of Introducing Talents of Discipline to University (B08026).

References

[1] Coëtmellec D., Lebrun D. and Ozkul C., Characterization of diffraction patterns directly from in-line holograms with the fractional Fourier transform, Applied Optics, 2002, 41, 312-319.
[2] Brunel M., Coëtmellec S., Lebrun D., Aït Ameur K. Digital phase contrast with the fractional Fourier transform, Applied Optics, 2009, 48, 579-583
[3] Brunel M., Shen H., Coëtmellec S., Lebrun D., Aït Ameur K., Femtosecond digital in-line holography with the fractional Fourier transform: application to phase-contrast metrology, Applied Physics B 2012, 106, 583-591
[4] Wichitwong W., Coetmellec S., Lebrun D., Allano D., Grehan G. and Brunel M., Long exposure time digital in-line holography for the trajectory of micronic particles within a suspended millimetrix droplet, 2014, 326, 160-165
[5] Coëtmellec S., Wichitwong G., Gréhan G., Lebrun D., Brunel M. and Janssen A.J.E.M., Digital in-line holography assessment for general phase and opaque particle, accepted in JEOS-RP Vol; 9 (2014)
[6] Lebrun D., Méès L., Fréchou D., Coëtmellec S., Brunel M. and Allano D., “Long-time exposure digital in-line holography for 3-D particle trajectography”, Optics express, Vol. 21 (20), 23522-23530 (2013)
[7] Glover A.R., Skippon S.M., and Boyle R.D. Interferometric laser imaging for droplet sizing: a method for droplet-size measurement in sparse spray systems. Applied Optics, 1995, 34, 8409-8421
[8] Shen H., Coëtmellec S., Gréhan G. and Brunel M. Interferometric laser imaging for droplet sizing revisited: elaboration of transfer matrix models for the description of complete systems. Applied Optics, 2012, 51, 22, 5357-5368
[9] Shen H., Coetmellec S., Brunel M. Cylindrical interferometric out-of-focus imaging for the analysis of droplets in a volume, Optics Letters 2012, 37, 3945-3947

[10] Shen H., Coetmellec S., Brunel M., Simultaneous 3D location and size measurement of spherical bubbles using cylindrical interferometric out-of-focus imaging, Journal of Quantitative Spectroscopy and Radiative Transfer, 2013, 131, 153-159
[11] Shen H.H., Saengkaew S., Gréhan G., Coetmellec S. and Brunel M., Interferometric out-of-focus imaging for the 3D tracking of spherical bubbles in a cylindrical channel, Optics Communications, 2014, 320, 156-161
[12] Brunel M., Shen H.H., Coëtmellec S., Gréhan G., and Delobel T., Determination of the Size of Irregular Particles Using Interferometric Out-of-Focus Imaging, Int. J. of Optics, 2014, ID143904, 8 pages
[13] Brunel M., Coetmellec S., Gréhan G. and Shen H.H., Interferometric out-of-focus imaging simulator for irregular rough particles, J. Europ. Opt. Soc., 2014, ID 14008
[14] Briard P., Saengkaew S., Wu X.C., Meunier-Guttin-Cluzel S., Chen L.H., Cen K.F. and Grehan G., Measurements of 3D relative locations of particles by Fourier Interferometry Imaging (FII), Optics Express, 2011, 19,13, 12700-12718
[15] Wu X.C., Meunier-Guttin-Cluzel S., Wu Y.C., Saengkaew S., Lebrun D., Brunel M., Chen L.H., Coetmellec S., Cen K.F. and Grehan G., Holography and microholography of particle fields: a numerical standard, Optics Communications, 2012, 285, 3013-3020
[16] Wu Y.C., Wu X.C., Saengkaew S., Meunier-Guttin-Cluzel S., Chen L.H., Qiu K.Z., Gao X., Grehan G. and Cen K.F., Digital Gabor and off-axis particle holography by shaped beams: a numerical investigation with GLMT, 2013, 305, 247-254